



GIS-based spatial landslide distribution analysis of district Neelum, AJ&K, Pakistan

Shah Naseer¹ · Tanveer UI Haq¹ · Abdullah Khan¹ · Javed Iqbal Tanoli¹ · Nangyal Ghani Khan¹ · Faizan-ur-Rehman Qaiser¹ · Syed Tallataf Hussain Shah¹

Received: 13 July 2020 / Accepted: 2 January 2021 / Published online: 23 January 2021
© The Author(s), under exclusive licence to Springer Nature B.V. part of Springer Nature 2021

Abstract

The Landslide happens in mountainous regions due to the catastrophe of slope through intensive rain and seismicity. The Himalayas is one of the susceptible parts of the world in the perspective of slope catastrophe hazard; i.e., Mass Movement, especially Neelum valley is considerable destruction of community infrastructure, highway, and critically disturbed the tourism segment. Landslide is a common and recurrent phenomenon in the northern mountainous terrain of Pakistan such as District Neelum. After the 2005 Kashmir earthquake, the importance of landslide investigation is increasing. The purpose of this research is to establish a brief landslide inventory and to determine the relationship of landslides with causative factors by spatial distribution analysis. With the aid of Google Earth imageries and field visits, a total of 618 landslides were identified in the study area of 3621 km. These landslide localities compared with causative factors. Finally, distribution maps are generated and analyse their feature class through Digital Elevation Model and ArcGIS. Landslide intensity is calculated in terms of landslide concentration. Landslide concentration (LC) is significantly found very high in slope gradient less than 30 (1.21) and the first 100 m zone around the road network (15.06). A bit higher landslide frequency is noted in east orienting slopes. In the first 100 m, zone road network and drainage networks are 83.49% and 62.78% of the total landslide occurs having LC value 4.6, respectively. The analysis shows that the steep slopes, an area closer to the road network, drainage network, barren lands, and Quaternary alluvium of loose material are more susceptible to landslides. In addition, a landslide classification map is also prepared on the basis of field observation that shows that debris slides are more dominating.

Keywords Concentration · Data · Function · Landslide · Spatial distribution · Slope

✉ Shah Naseer
shahnaseer125@gmail.com

¹ Department of Earth Sciences, COMSATS University Islamabad, Abbottabad, Pakistan

² Institute of Geology, University of Azad Jammu and Kashmir, Azad Kashmir, Muazaffarabad, Pakistan

1 Introduction

The Himalayan belt due to its, topography, geology, environment, and massive tectonic activity, is susceptible to landslide (Sarwar et al. 2016). It has been considered that 30% of the world landslide happen in these Himalayan series (Khan 2000). The Neelum District lies in the northeast of the Muzaffarabad and is the part of lesser and higher Himalayan Pakistan.

The word landslide refers to the downward movement of a rock mass, debris, or earth under the influence of gravity (Cruden and Varnes 1996). Various triggering factors like intense rainfall, earthquake, and anthropogenic activity cause landslides. In developing countries like Pakistan, a landslide is one of the major disasters responsible for fatalities, damages of the communication links, loss of fertile soil, and economic losses in the mountainous areas (Jadoon et al. 2015; Petley et al. 2006). Particularly, northern part of Pakistan such as Neelum district, AJ&K lies the part of lesser and higher is characterized by steep slopes (Sato et al. 2007), active tectonics, fragile rocks units, and heavy monsoon rains that makes the area more prone to landslide. This instability has caused many slope failures in the region. Particularly, the slope failures occur mainly along the main road built in the mountain environment (Ali et al. 2017). In addition, deforestation has further accelerated the problem of mass wasting in the region (Basharat 2012; Kamp et al. 2008; Owen et al. 2008; Sudmeier-Rieux et al. 2007).

In Pakistan, landslides occur regardless of the time frame and slope parameters for its geomorphological and climatic conditions. Nevertheless, its existence becomes more conspicuous by the elements of high values economically downslope such as casualties, economic losses, and injuries (Tan et al. 2020). Especially, the Northern area of Pakistan which is prone to severe landslide because of the young Himalayas and throughout the active fault zone. The most critical fault line exists and stretches as far as in the study area, which making the area highly prone to natural disasters, including landslides.

The Neelum road is the main connected path with interior districts of Kashmir and Pakistan. The road has been badly affected due to landslide during the rainy season and cause road blockage many days to weeks. The blockage effects the life and tourism sector. A huge number of the landslide were also triggered along this highway during the 2005 (Basharat and Rohn 2015) Kashmir earthquake which causes blockage of the road for many days (Basharat 2012). The Donga Kass and Panjgran, landslide were the most significant that reactivated during the 2005 Kashmir earthquake along this road (Basharat and Rohn 2015).

To reduce the effect of landslides, avoidance is the most useful mitigation measure (Hussain et al. 2017). Therefore, modern, and emerging techniques like digital elevation model (DEM), high resolution satellite data, and geographic information system (GIS) are very useful for hazard analysis, landslide susceptibility mapping, and risk assessment. Establishment on the result of these observations, mitigation measures such as structural measures (check dams, debris basins) or non-structural measures could be taken to reduce the risk (Ayalew and Yamagishi 2005). In order to minimize the damages due to mass movement in the future, this study has focused on producing a GIS-based landslide distribution maps and analysis with respect to many geological and topographical factors (Regmi et al. 2016) for district Neelum. The present study focused to understand active landslide, investigate the mountain geomorphic hazards distribution probability by assembling historical landslide evidence (Zhou et al. 2020). This study is the first attempt and will contribute as a primary database for future landslide research

in this area. In addition, it will be helpful for planners and other concerned authorities to mitigate the landslide hazards in the region (Fig. 1).

2 Materials and methods

2.1 Study area

The study area is mainly hilly and mountainous with valleys and stretches of plains (Bouhadad et al. 2010; Kiani et al. 2005) The elevation ranges between 730–3600 m (Fig. 2). The steep slopes and escarpments are prominent features of the area. The entire region is drained by the Neelum River and its tributaries. Due to extremely difficult terrain, the Valley is divided by its forested, north facing left bank (Sudmeier-Rieux et al. 2007). The right bank is South-facing to a large extent deforested.

2.2 Geology and tectonic setting

The area comprises of lesser to higher Himalayas (Fig. 3). Rocks of lesser Himalayas have composed of Precambrian Tanol Formation intruded by the (Mughal et al. 2016) Cambrian Mansehra—type granites (Calkins et al. 1975; Wadia 1931) and Tectonically, the main boundary thrust (MBT) demarcates the boundary between the lesser and the Sub-Himalayas at Nauseri area. The rock units of the Sub-Himalayas are composed of sedimentary sequences (Greco 1989; Hutchinson 1988; Naseer et al. 2019; Pierson et al. 1993) and extend to the southern end of the study area. The general strike direction in the area between Tithwal and Kel is northwest-southeast. The general dip direction from Titwal to

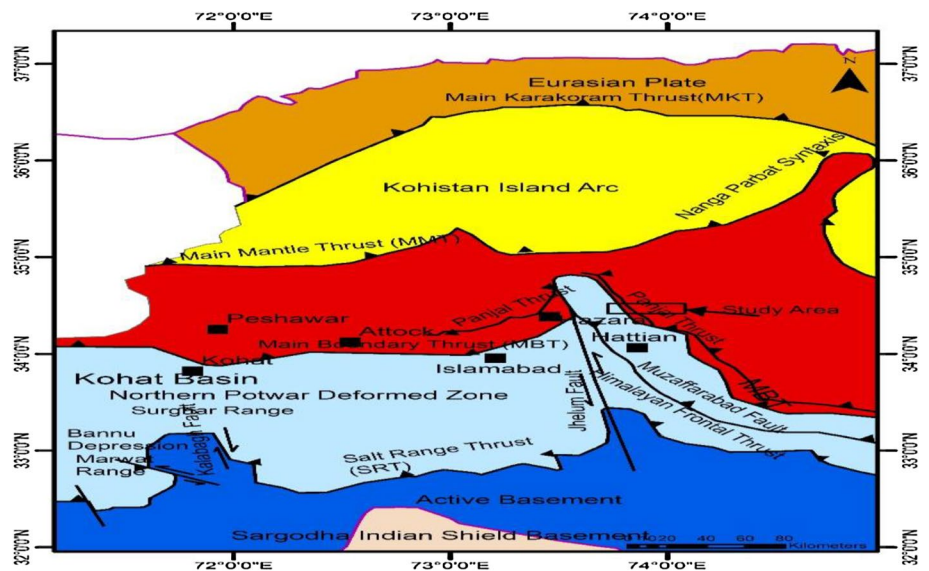


Fig. 1 the regional tectonic map shows the major tectonics features in northern Pakistan (compiled after (Baig and Lawrence 1987; Basharat 2012; Wadia 1931)

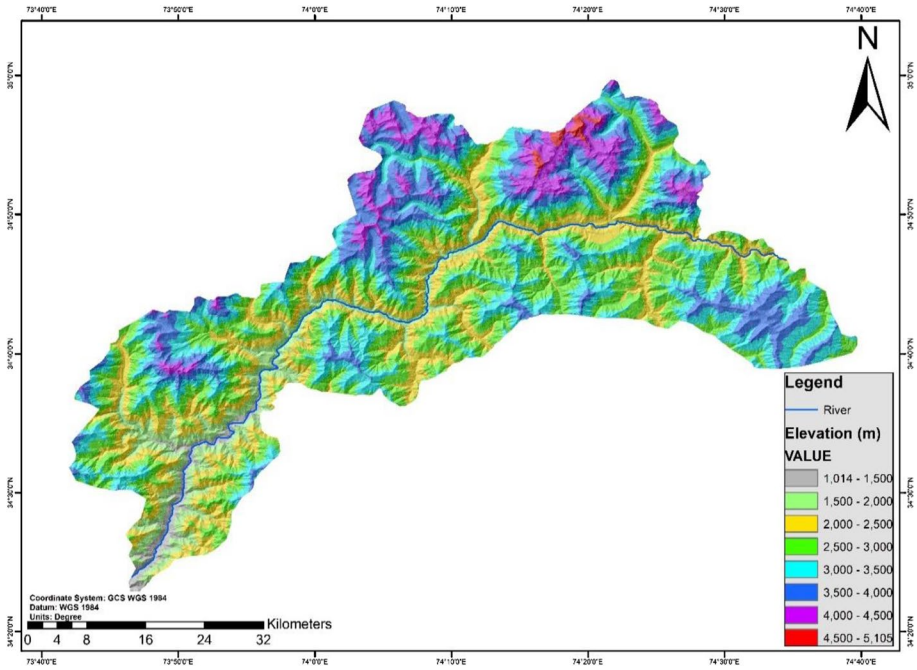


Fig. 2 Digital elevation model (DEM) of the study area

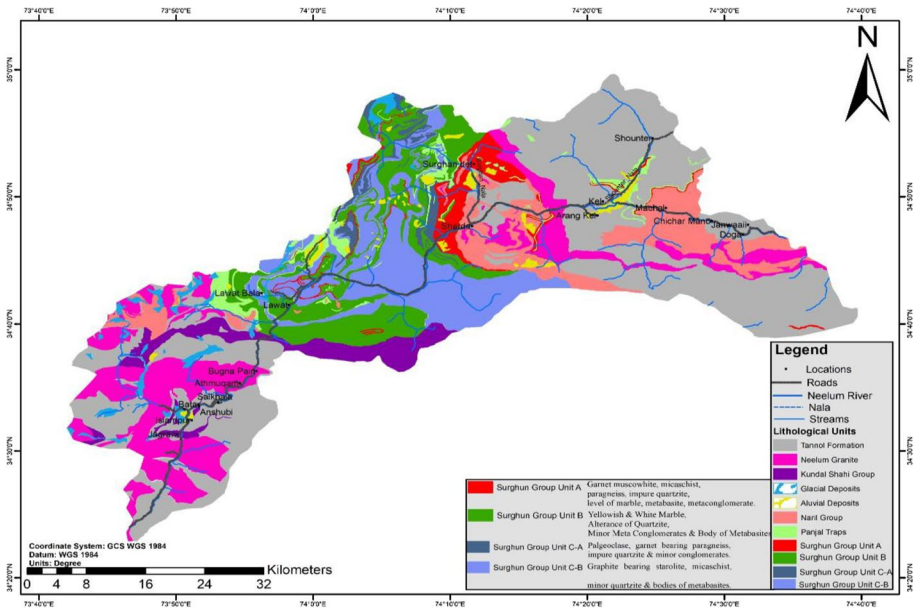


Fig. 3 Geological map of the study area (Source: AKMIDC)

Salkhala village is northeast and from Salkhala to Kel, the general dip is in the opposite direction i.e., southwest. There is a distinct syncline, the Salkhala syncline, between the villages of Shahkot and Salkhala with its axis running east–west and plunge toward east. Folds are generally open parallel type which is not noticeable features in the area. There are noticeable faulted contacts such as Barrayn, Bata, Lala and Loat Fault.

3 Data

3.1 Data collection

Initially, previous literature regarding landslide spatial distribution was collected and thoroughly reviewed.

A variety of research techniques was used to collect field data. Prior to the fieldwork, topographical and geological maps were collected (Kanwal et al. 2017). To obtain the expected results, questionnaires were designed to collect information regarding locally understood causes within the study area. Most of the data were obtained through a questionnaire survey and observations during field trips.

Landslides were marked using different conventional and new emerging (Shafique et al. 2016) techniques i.e., field visits and remote sensing technologies. Google earth image-ries and satellite imagery were used to identify landslides in the study area which were not accessible through field surveys. Hence, a brief landslide inventory was prepared using ArcGIS. Then, different causative maps like slope, aspect, curvature, elevation, and drainage were derived from the SRTM digital elevation model (DEM) (Fig. 4).

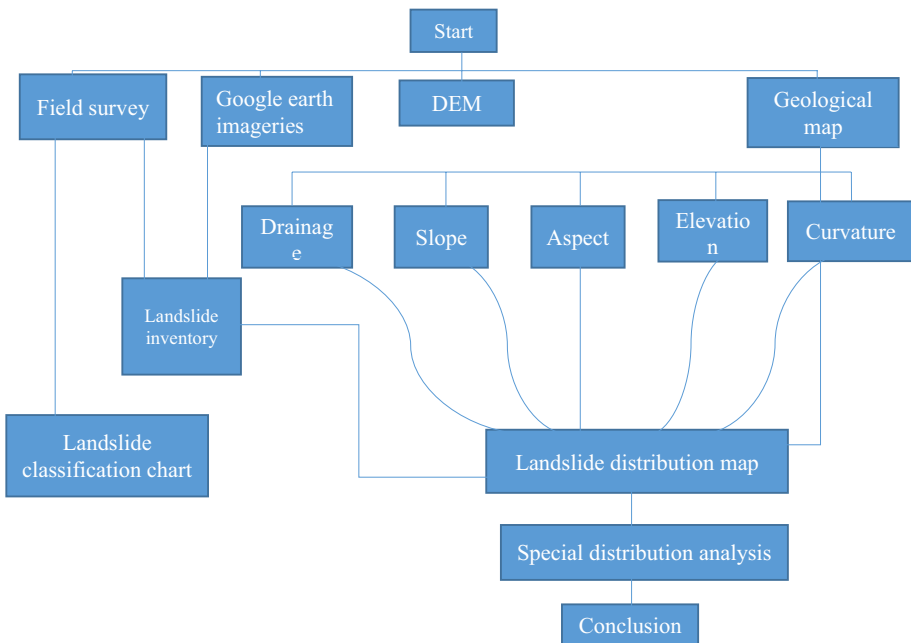


Fig. 4 Process flow diagram of the research work

3.2 Landslide inventory

The landslide inventory of the study area was prepared based on field investigation as well as by the visual interpretation of Google imageries (Sato et al. 2007). The final landslide inventory contains 618 landslides out of them 138 landslides were marked during field visits. These landslides were converted from polygons to point feature in ArcGIS for spatial distribution analysis. Most of the landslides were found along drainage and road network in the study area because all these geo-environmental and human factors have a great deal in triggering of landslides (Bibi et al. 2016) (Fig. 5).

3.3 Landslide special distribution analysis

The data development is the first step before performing special data analysis to contract landslide causative factors. To develop a different factor map, for that, some of the previous data are carried out according to its own purpose. Preparation of landslide spatial distribution map concerning different geo-environmental factors involves large data sources. Therefore, performing spatial analysis requires a spatial database for the study area, and a variety of software was involved for achieving certain valuable information. Geographic information system (GIS) 10.4.1 was used for mapping, digitization, and analyzing the data collected from various sources. Data in the form of tables and flow charts were prepared and presented by using MS office. The location of landslide and attribute data is organized firstly in MS Excel for graphical representation.

The maps are obtained by various sources were scanned and saved in JPEG or TIFF format having no spatial reference. Therefore, to make these maps spatially recognized, geometric corrections were applied according to the world geodetic system 1984 (WGS 84). After geo-referencing, these maps are transformed into Projected Coordinate system UTM zone 43 N to get the distances in the meter for some map analysis like slope map, fault and drainage buffers, etc. Then correlation was carried out between

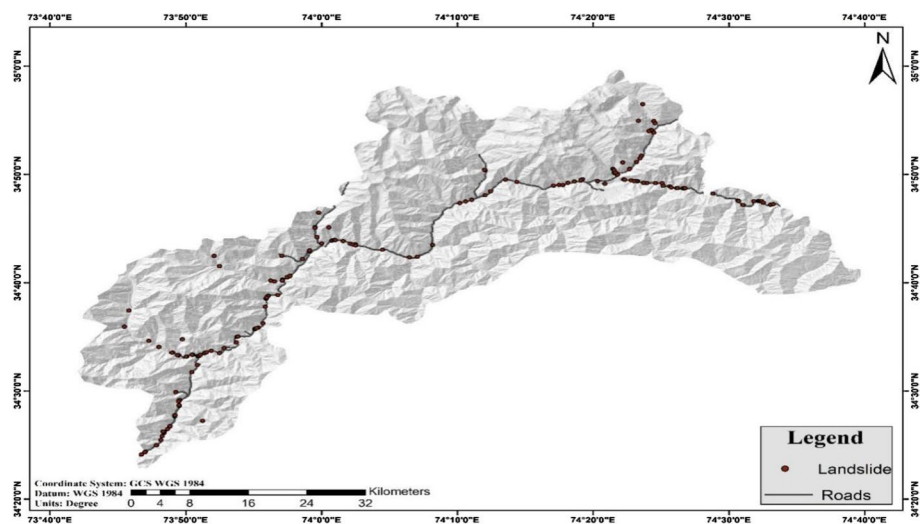


Fig. 5 Landslide inventory illustrates distribution of landslides within the study area

geological units and topographic factors like slope, aspect, elevation, curvature, drainage, etc. Many distribution maps were generated concerning each causative factor.

The digital elevation model (DEM) of 12.5 m resolution, for developing the factor map by using “Spatial Analyst” to make elevation, slop, aspect, and curvature maps. Some of the calculations are made to estimate the area in km² of each feature class i.e., slope category, elevation range, land use type, etc.

$$\text{Area in km}^2 = \text{No. of pixels per class} \times 0.0001563.$$

Hence, no. of pixels containing each feature class of the causative factors is multiplied with the above factor to calculate the area in a square kilometer.

3.4 Elevation

Elevation plays most important role in slope failures, and the Neelum district has a higher altitude elevation at higher altitudes the weathering process become more intense due to heavy precipitation in addition to the frost action caused by drop and temperature, so landslide concentration can be expected more (Norini et al. 2016; Waseem et al. 2018) A larger part of the study area lies between the elevations from ranges 1500 to 4500 m (Fig. 6). Some higher peaks more than 4500 m are also present. The minimum elevation of the area is 1014 m, and the maximum elevation is 5105 m.

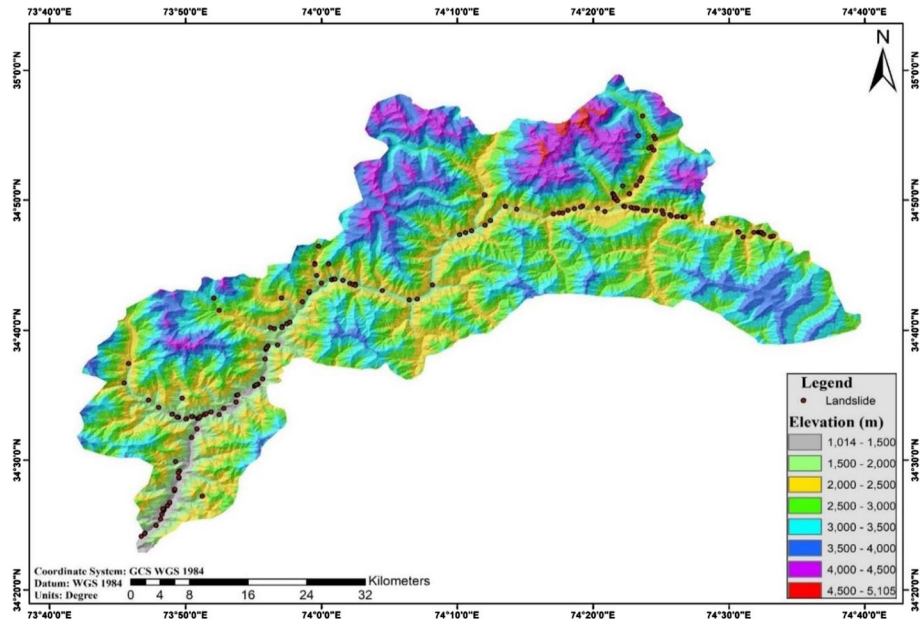


Fig. 6 Map showing distribution of landslides with respect to elevation of study area

3.5 Slope gradient

It is also the main factor of landslide occurrence. If the slope angle is gentle, the shear stress will be low effective and landslide frequency will be expected low (Sandyavetri 2016). And if the angle is steeper it will be more effective of shear stress. In the present study, slope gradient map was prepared from SRTM (DEM) by using ArcGIS software. The gradient was classified into eight classes having interval i.e., 10 (Fig. 7).

3.6 Slope aspect

Slope aspect is also another causative factor of slope instabilities (Brawner and Wyllie 1976), as the orientation of the slope controls the ground surface to some certain weathering agents and in winter seasons the alternate process of frost thawing and subsequent melting on the exposure of the surface to sunlight which is control by slope orientation (Romana 1985). Slope aspect usually represents the direction facing of the terrain surface. A Slope aspect map was prepared from SRTM (DEM). The aspect was classified into eight classes using ArcGIS (Fig. 8).

3.7 Slope curvature

The curvature of the slope shows the shape of the slope. It is one of the controlling factors for slope failure (Nefeslioglu et al. 2008). Where slope failure occurs, Curvature is responsible for the geometry of slope (Abbasi et al. 2002), water concentration or run off spreading becomes a vital cause of shallow sliding depend upon the curvature of the area (Baig and Lawrence 1987; Xu et al. 2014).

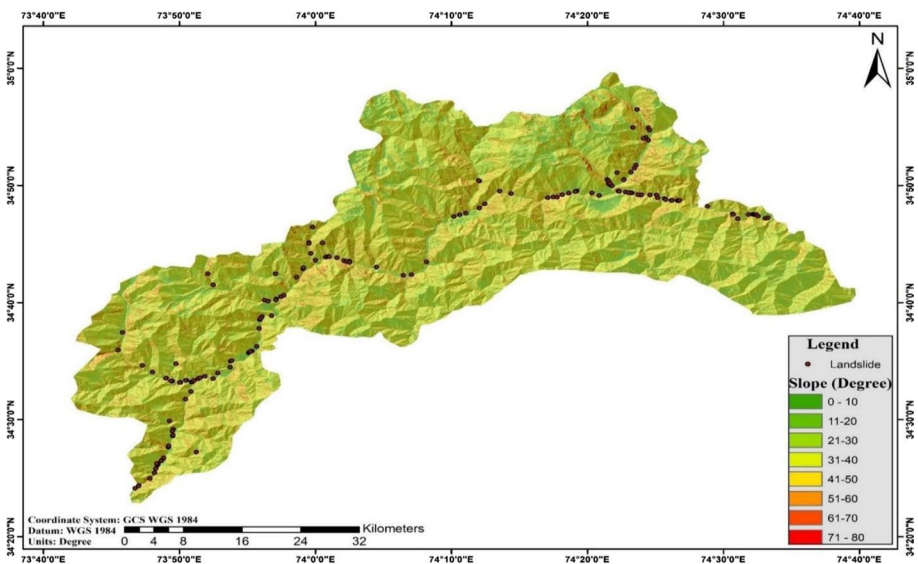


Fig. 7 Map shows distribution of landslides with respect to different slope classes of study area

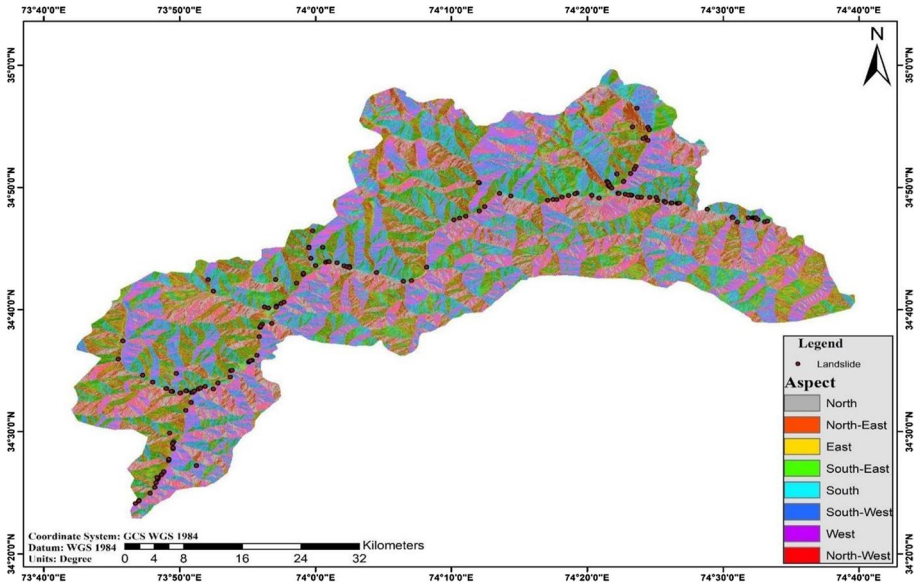


Fig. 8 Map shows distribution of landslides among different slope orientation

Slope curvature also controls the flow of water along slope (Ayalew et al. 2004). Curvature standards were comprehensively used for intersection plane surface. The curvature analysis permits categorizing the part into concave and convex to identify regions that are prone to mass movements. A positive curvature value specifies an upwardly convex surface while the negative specifies an upwardly concave surface. The curvature map and profile curvature map were created in ArcGIS. One class is convex which shows positive values, and the other class is concave which shows negative values (Fig. 9).

3.8 Distance to drainage

Distance to stream or drainage is also considered as another causative factor of land sliding because groundwater movement in hilly areas cuts the toe frequently (Sudmeier-Rieux et al. 2007). The study area is comprised of a large drainage network. The drainage network of the region was extracted from the digital elevation model (DEM) by using Arc GIS environment through Watershed analysis. In the extracting procedure calculate Fill, Flow Direction, and then Flow Accumulation with the help of Spatial Analyst Tool and Hydrology Tool in GIS. The Flow Accumulation map is the visualization as a drainage pattern.

To assess the influence of hydrological network and landslide concentration in the study area, a classified map was prepared having different zones of increasing distance from the drainage network (Fig. 10).

3.9 Distance to road

Road network is also a causative factor of landslide occurrence (Sudmeier-Rieux et al. 2007; Yalcin et al. 2011) Excavation for roads development and moment of transport

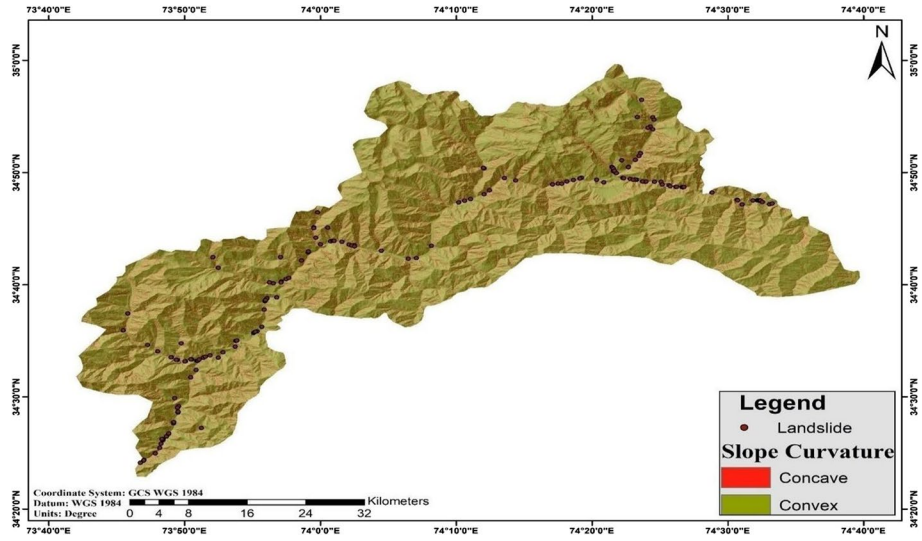


Fig. 9 Map shows distribution of landslides with respect to curvature

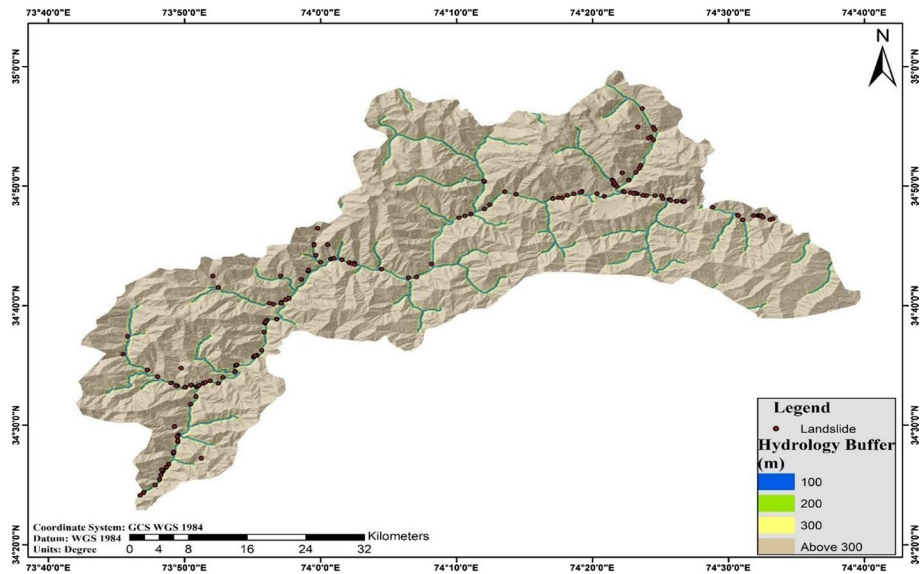


Fig. 10 Map shows distance of landslides from drainage network

vibrate the unstable steep slopes in a hilly area, which causes slope failure (Highland and Bobrowsky 2008; Sato et al. 2007). To locate its bearing on slope stability, the road map was appropriately digitized using a topographic sheet of Neelum district, Kashmir on the scale of 1:500,000 prepared by the Geological Survey of Pakistan. Consequently, a highway buffer map was prepared through GIS (Fig. 11).

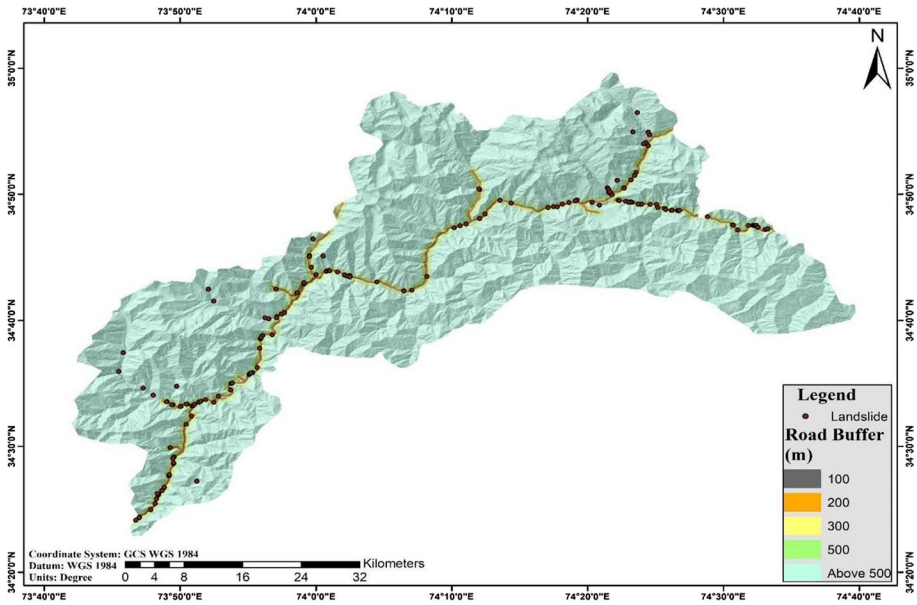


Fig. 11 Map shows distribution of landslides from their proximity to road networks

3.10 Lithology

Landslide is also dependent on the nature of rock units. Generally, the majority of landslides occur in formations having loose or fragile lithology that give ease in mass movements (Norini et al. 2016). To determine the relationship of landslide occurrence with lithology.

The study area mainly consists of eleven lithostratigraphic units in which the Precambrian Naril Group covers 9.75%, Precambrian Tannol Formation covers 36.33%, Precambrian Kundal Shahi Group covers 4.31%, and the Upper Paleozoic to Mesozoic Surhgung Group covers 29.01% of the study area. The Neelum granite cover 14.29% of the study area. The Glacial Deposits cover 1.93% while the alluvial deposit covers 1.44% of the study area (Fig. 12).

4 Results and discussion

4.1 Landslide classification

Landslide classification is carried out by field observation. These are classified based on nature of movement and material involved (Cruden and Varnes 1996), and a classification map is prepared. The study area mainly comprises debris slides, followed by a rockslide, rock fall, and debris fall (Table 1). Figure 13 shows comparison of different landslide types and their %age. Debris slide is the most dominated landslide type in the study area. Because of quick actions of weathering and erosion (denudation) in hilly

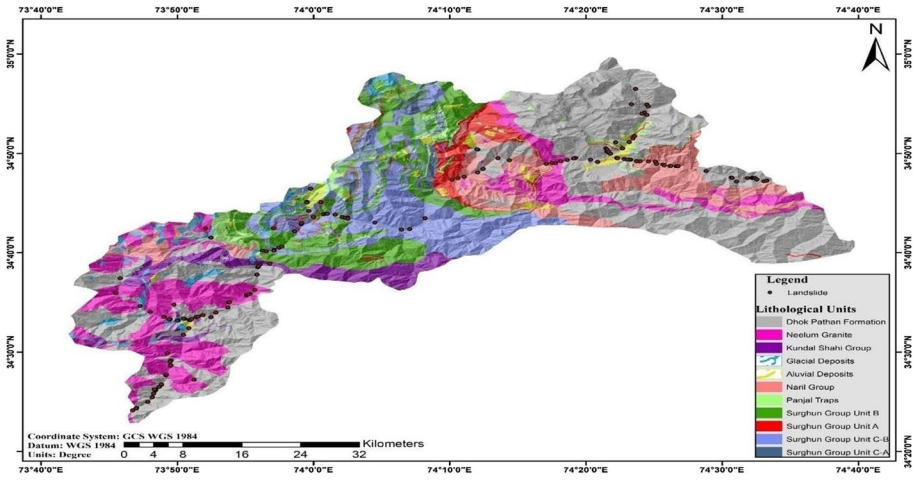


Fig. 12 Map showing distribution of landslides with respect to geology

Table 1 Landslide type in the study area

Slide types	No. of landslides	% of total landslides
Debris sfiglide	79	57.24
Rock slide	26	18.84
Debris fall	19	13.76
Rock fall	14	10.14
Total	138	100

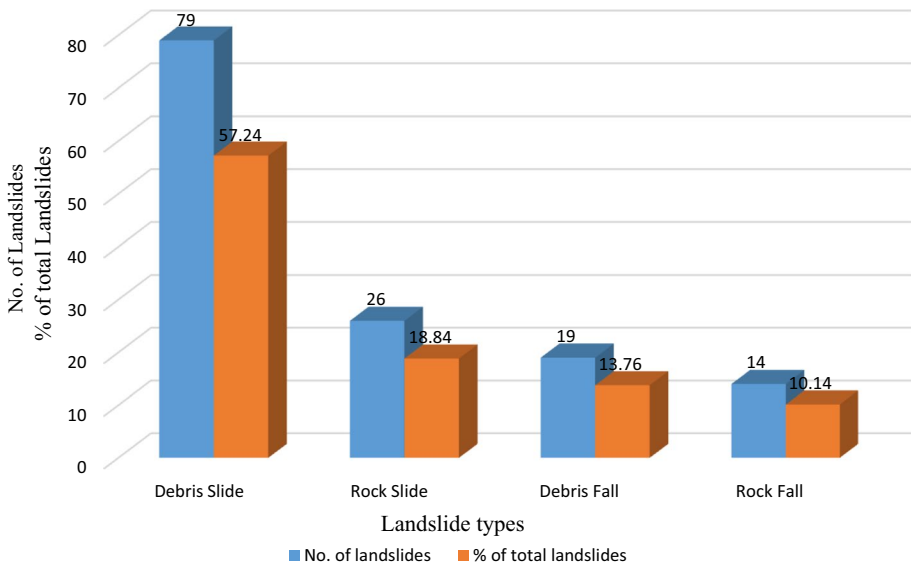


Fig. 13 Graph chart shows dominance of different landslide types

terrain, a good amount of thick soil and regolith is produced which is further dislocated as debris slide.

4.2 Spatial distribution analysis

After establishing a brief landslide inventory (Shafique et al. 2016) by field visits and Google Earth imageries, the analysis of these landslide occurrence was carried out by different causative factors including geological and topographic factors with the aid of distribution maps. The results of these spatial distribution analysis are given in detail below.

4.2.1 Landslide concentration (LC) as a function of slope gradient

The relationships between slope angle and landslides are shown in Table 2 and Fig. 14. Most landslide occurrence (33%) is in a slope of 21–30°. The second highest landslide occurrence (29.77%) is in a slope of 31–40°. The slope classes of 11–20 and more than 41–50 have an equal percent age of landslides i.e., 12.62%. And above 60° it reduces to only 0 to 0.97%. The analysis shows that most of the landslides (62.77%) have occurred in low to moderate slope (Xu et al. 2014) i.e., 21–40°. In case of high slope angles, the weight of slope material directly and efficiently transformed to the ground by the toe, and slope stays stable unless (Buss et al., 1995) any strong activity occurs or toe removal takes place by any natural or human activity (Taherynia et al. 2014). The Landslide concentration ratio has the highest value (0.47) in 0–10°. And declines to 0.378 in 21–30°, 0.371 in 0–10° and declines to 0.378 in 21–30°, 0.371 in 11–20°, 0.33 in 51–60°, 0.29 in 61–70°, 0.24 in 31–40°, and 0.18 in 41–50.

4.2.2 Landslide concentration as a function of elevation

In the present study, a factor map of elevation was classified into eight classes as shown in Table 3 and Fig. 15. The analysis of landslide and elevation reveals that most landslides events (36.89%) occurred at the elevation between 1014–1500 m. While, the other prominent elevation classes in decreasing order of landslide occurrence are 2000–2500 m (31.06%), 1500–2000 m (29.12%), 2500–3000 m (2.58%), 3000–3500 m (0.32%), 3500–4000 m (0%), the elevation class 4000–4500, and 4500–5105 m. Most

Table 2 Relationship between landslides and slope angle

Slope (°)	Area (km ²)	Area %	Land Slides	L.S %	L.S concentration
0–10	58.54	2.75	28	4.53	0.47
11–20	210.18	9.89	78	12.62	0.37
21–30	539.37	25.4	204	33	0.37
31–40	740.29	34.86	184	29.77	0.24
41–50	432	20.34	78	12.62	0.18
51–60	120.89	5.69	40	6.47	0.33
61–70	20.6	0.97	6	0.97	0.29
71–80	1.47	0.06	0	0	0
Total	2123.38	99.96	618	99.98	2.25

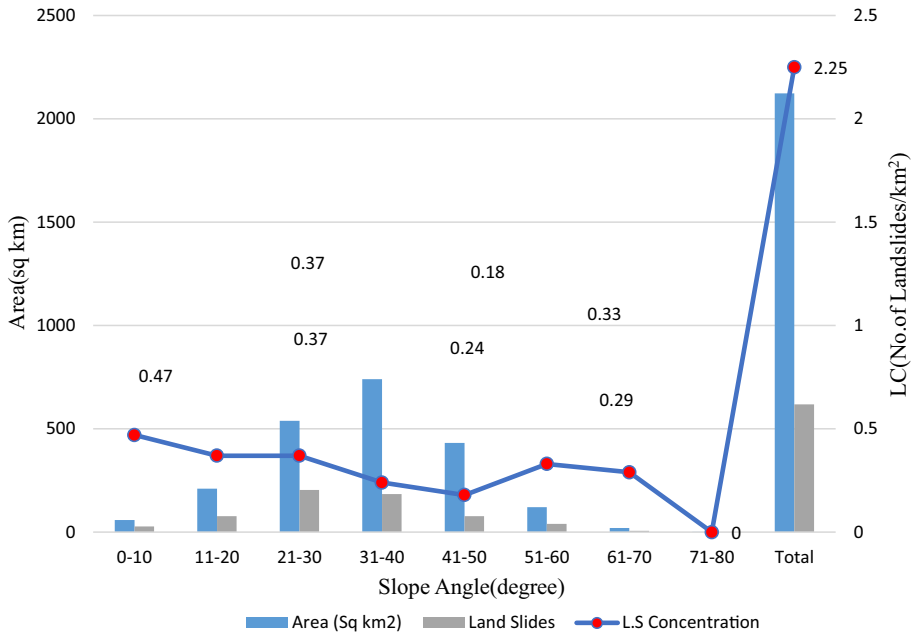


Fig. 14 Spatial distribution analysis of landslides with respect to slope gradient

Table 3 Relationship between landslides and elevation

Elevation (m)	Area (km ²)	Area%	Land Slides	L.S%	L.S concentration
1014–1500	45.87	2.16	228	36.89	4.97
1500–2000	165.53	7.79	180	29.12	1.08
2000–2500	407.66	19.19	192	31.06	0.47
2500–3000	579.94	27.31	16	2.58	0.02
3000–3500	475.75	22.4	2	0.32	0
3500–4000	310.74	14.63	0	0	0
4000–4500	127.19	5.99	0	0	0
4500–5105	10.65	0.5	0	0	0
Total	2123.33	99.97	618	99.97	6.54

of the landslides have occurred in elevation range from 1014 to 2500 m (97.07%). While at higher altitudes collectively comprise only 2.9% of total landslides.

Landslide concentration ratio has the highest value (4.96) in 1014–1500 m. And declines to 1.08 in 1500–2000 m, 0.47 in 2000–2500 m, 0.02 in 2500–3000 m, 0.004 in 3000–3500 m, and the elevation 3500–5105 m. At lower altitude, landslide concentration is high, this is due to the fact of main road networks and major streams of the area which lie in this zone and are influential causes for landslide occurrence (Sandyavritri 2016).

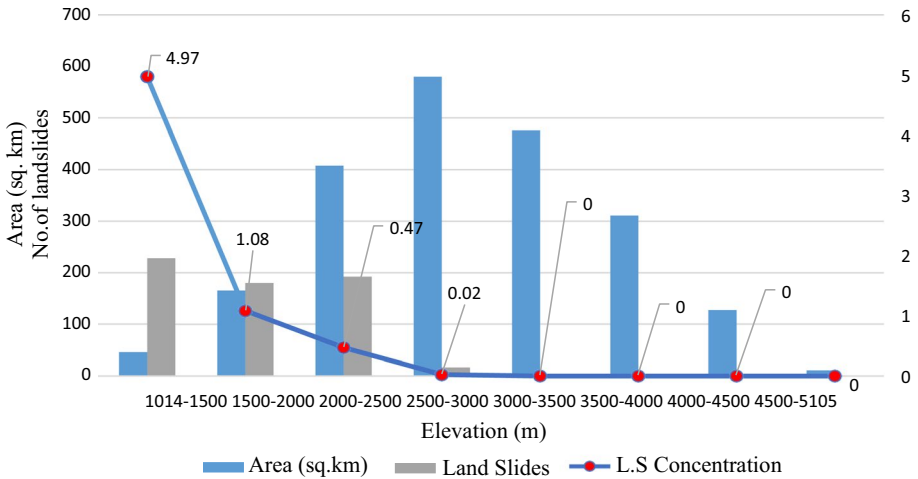


Fig. 15 Spatial distribution analysis of landslides with respect to elevation

4.2.3 Landslide concentration as a function of slope aspect

The aspect analysis of the study area shows that it comprises more or less an equal amount of area in all orientation categories. However, east orienting slopes are a little more than other orientations (Barredo et al. 2000); followed by the southeast and north-east directions (Table 1).

Most of the landslides (27.83%) have occurred in the east direction; followed by the southeast (24.91%), south (22.97%), southwest (11.97%), northeast (7.44%), north (3.55%), the west has equal% to the northwest (0.647) (Table 4).

The highest landslide concentration (1.18) is also found in eastward orienting slopes and gradually declines in the southeast (1.17), northeast (1.04). It has the same value of 1.00 in southwest and west directions, then it declines to the south (0.92), northwest (0.79), and north (0.63) (Fig. 16).

Table 4 Relationship of landslides with slope aspect

Slope aspect	Area (km ²)	Area%	Land slides	L.S%	L.S concentration
N	249.87	11.76	22	3.55	0.08
NE	234.76	11.05	46	7.44	0.19
E	310.1	14.6	172	27.83	0.55
SE	310.99	14.64	154	24.91	0.49
S	282.73	13.31	142	22.97	0.5
SW	275.7	12.98	74	11.97	0.26
W	235.58	11.09	4	0.647	0.01
NW	223.6	10.53	4	0.647	0.01
Total	2123.33	99.96	618	99.964	2.09

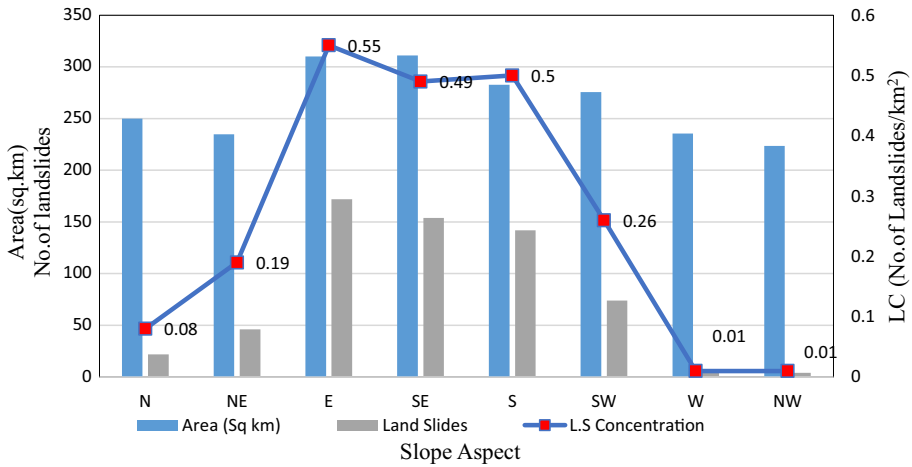


Fig. 16 Spatial distribution analysis of landslides with respect to slope aspect

4.2.4 Landslide concentration as a function of slope curvature

The curvature of the study area was classified in two classes. Most of the study area lies in convex curvature i.e., 81.67% of the total area. While 18.32% of the area has a concave curvature. Spatial relationships between landslide and curvature shows that more landslides occur on the convex side (70.87%) as compared to that of concave curvature (29.12%) (Table 5). Spatial distribution analysis of curvature and landslides are shown in Figs. 14 and 15. Landslide concentration is 0.46 in concave slope, and it decreases to 0.25 in convex slope.

4.2.5 Landslide concentration as a function of lithology

Precambrian Tannol Formation covers 36.33% of the study area, Precambrian Naril Group covers 9.75%, Precambrian Kundal Shahi Group cover 4.31%, and the Upper Paleozoic to Mesozoic Surhgun Group covers 29.01 of the study area. The Neelum granite covers 14.29% of the study area. The Glacial Deposits covers 1.93% while the alluvial deposit covers 1.44% of the study area Fig. 17.

Highest number of landslides (46.60%) are found in the Tannol Formation which is the most dominant rock unit of the study area. The second most landslide occurrence (15.53%) is in Neelum Granite. The third lithological unit concerning landslide dominance is Naniyal group/Surgan Group Unit C–B having 9.70% of the total landslides. Surgan Group Unit B

Table 5 Relationship of landslides with slope curvature

Curvature	Area (km ²)	Area%	Landslides	L.S%	L.S Concentration
Concave	389.16	18.32	180	29.12	0.46
Convex	1734.21	81.67	438	70.87	0.25
Total	2123.37	99.99	618	99.99	0.71

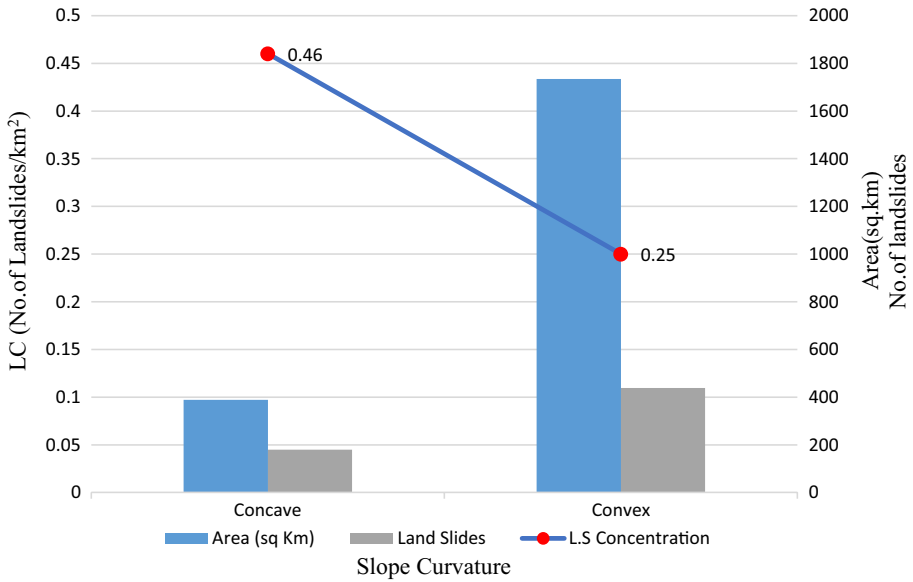


Fig. 17 Spatial distribution analysis of landslides with respect to slope curvature

comprises 5.50% of the total landslides while the Glacial Deposit/Punjat Trips of 2.91% of the total landslides and the Alluvial Deposite/ Surgan Group Unit A having 2.58% of the total landslide. The Kundal Shahi Group having 1.94% of the total landslides while Surchan Group Unite C–B having 0% of the total landslide (Table 6). Landslide concentration sharply fluctuates in all rock formations because each rock unit has distinct physical properties that assist or resist slope failures. The highest landslide concentration is in the alluvial deposit (0.521) because of its loose matrix and unstable binding framework

Table 6 Relationship between landslides and lithological unit

Geological units	Area (km ²)	Area%	Landslides	L.S%	L.S concentration
Tannol formation	771.53	36.33	288	46.6	0.37
Neelum granite	303.48	14.29	96	15.53	0.31
Kuldani Shai group	91.7	4.31	12	1.94	0.13
Glacial deposit	41.11	1.93	18	2.91	0.43
Alluvial deposit	30.69	1.44	16	2.58	0.52
Naril group	207.03	9.75	60	9.7	0.28
Punjat traps	61.15	2.87	18	2.91	0.29
Surgan group unit A	69.33	3.26	16	2.58	0.23
Surgan group unit B	237.38	11.17	34	5.5	0.14
Surgan group unit C-B	268.15	12.62	60	9.7	0.22
Surgan group unit C-A	41.79	1.96	0	0	0
Total	2123.34	99.93	618	99.95	2.92

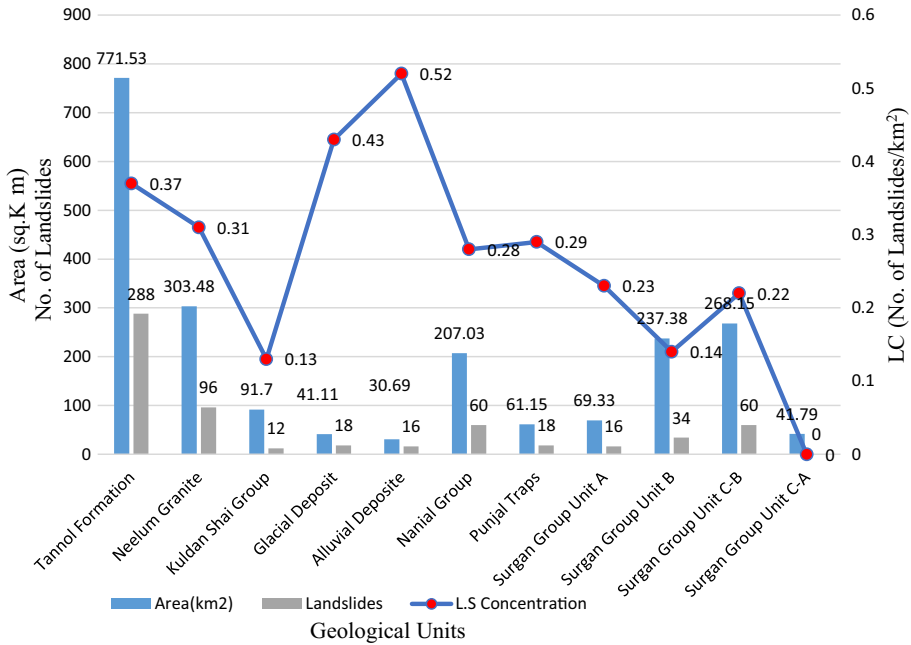


Fig. 18 Spatial distribution analysis of landslides with respect to lithological units

Table 7 Relationship between landslide and their distance to drainage

Drainage (m)	Area (km ²)	Area%	Land slides	L.S%	L.S concentration
100	84.18	3.96	388	62.78	4.6
200	83.45	3.93	90	14.56	1.07
300	80.39	3.78	10	1.61	0.12
above 300	1875.34	88.31	130	21.03	0.06
total	2123.36	99.98	618	99.98	5.85

it is more prone to landslides. The lowest landslide concentration is in Kudan Shai Group (0.13) (Fig. 18).

4.2.6 Landslide concentration as a function of distance to drainage

Drainage network effects significantly in slope destabilization in hilly areas as streams cause undercutting of slope toes, and all drainage channels cause percolation of surface waters to the ground which is also responsible for slope destabilization especially where expansive clays are present (Agliardi et al. 2009).

To understand the influence of drainage on land sliding, a map is prepared to shows increasing distance zones with intervals of 100 m, 200 m, 300 m, and more than 300 m. In the first 100-m interval, 62.78% of the total landslides occur. In the next 100 m, 14.56% of the total landslides occur and in the area of 200 m to 300 m around drainage, 1.16% of the total landslides occur (Table 7). The area above 300 m is considered as one class and about 21.03% of the total landslide is occurring in this zone. In the first 100 m around drainage,

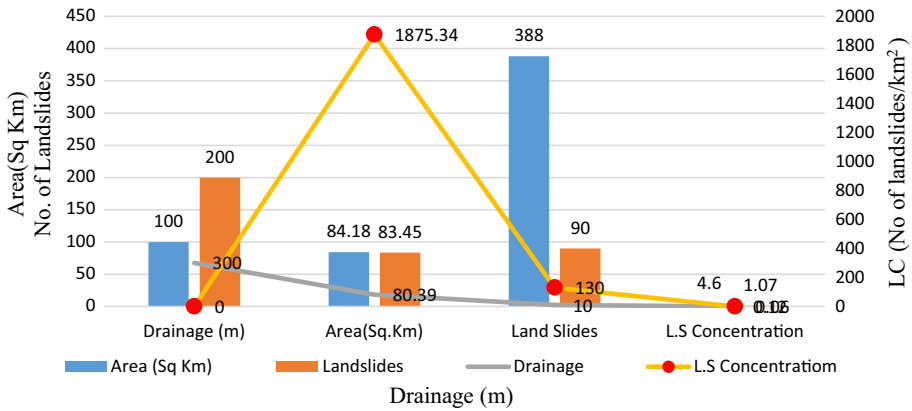


Fig. 19 Spatial distribution analysis of landslides with respect to distance from drainage network

Table 8 Relationship between landslide and their distance to road network

Road (m)	Area (km ²)	Area%	Land slides	L.S%	L.S concentration
100	34.26	1.61	516	83.49	15.06
200	32.66	1.53	30	4.85	0.91
300	31.75	1.49	8	1.29	0.25
500	61.7	2.9	12	1.94	0.19
Above 500	1962.98	92.44	52	8.41	0.02
Total	2123.35	99.97	618	99.98	16.43

the landslide concentration is 2.07, and then regularly declines to 1.18 in the 200 m zone, 0.82 in the 300 m zone, and 0.62 in the more than 300 m zones (Fig. 19). As a result, landslide concentration is significantly high near to drainage network.

4.2.7 Landslide concentration as a function of distance to road network

Human activities also cause significant slope destabilization in developing countries especially the roads that are built in a hilly area cause more ground failures as slope toes are instantly removed which causes sudden or gradual failures of ground (Hewitt 1999). To understand the effect of road networks over landslide distribution, a classified map of the road network was prepared to estimate the impact of distance to the roads. For better evaluating the role of roads in slope failure, four multiple buffers were developed along the roads. The developed buffer zones are 100 m, 200 m, 300 m, 500 m, and > 500 m from the roads. The first 100 m buffer encircles 1.613% of the total study area. 100–200 m buffer covers 1.538% of the study area. 200–300 m buffer covers 1.495% of the total study area. Next 300–500 m buffer covers 2.906 and above 500 m, 92.446% of the study area lies (Table 8). Only in the first 100 m distance 83.49% of the total landslides occurs, in the next 100 m buffer zone landslide%age declines to only 4.85. In 300 m buffer from roads, only 1.29% of the total landslides occurs. 500 m distance from the road network, only 1.9% of

the total landslide occur. Above 500 m distance from all the area is classified as one cumulative class, and 8.41% of the total landslides occur in this class (Table 8).

In the first 100 m buffer, landslide concentration is 15.058 and in the next zone of 200 m, it declines to 0.918. In the next 300 m it reduces 0.25, in next 500 m. It further reduces 0.194 and in the zone of more than 500 m, it slightly decreases to 0.026 (Fig. 20). Generally, landslide concentration has the highest landslide concentration near to the roads and shows a sharp decrease in moving away from the roads. This phenomenon is due to the disturbance created by human activities in road building which caused the imbalance of slope equilibrium by cutting the toes of steep mountainous terrain. And triggered a greater number of landslides near the road network. Away from the road network, the ground is more stable and safe as landslide concentration is very low.

5 Discussion

Abundant measures and practices are used for landslide distribution modeling. Nevertheless, the greatest informal to use and comprehend performances with high precision provide outstanding landslide models. GIS-based approaches are accomplished for considerable calculation rate marked through the results of the current study.

This study was an effort to produce a landslide hazard distribution map by using digital elevation models (DEM), for simply extraction Geological and Geomorphic statistics supplementary with landslides. We make a comprehensive field study and analysis to preparing reliable and valuable material for landslide distribution hazard inventory.

In the present study, the method of landslide spatial distribution analysis is too applied to determine and sort out different strongly influential causative factors that caused slope failures (Brawner and Wyllie 1976).

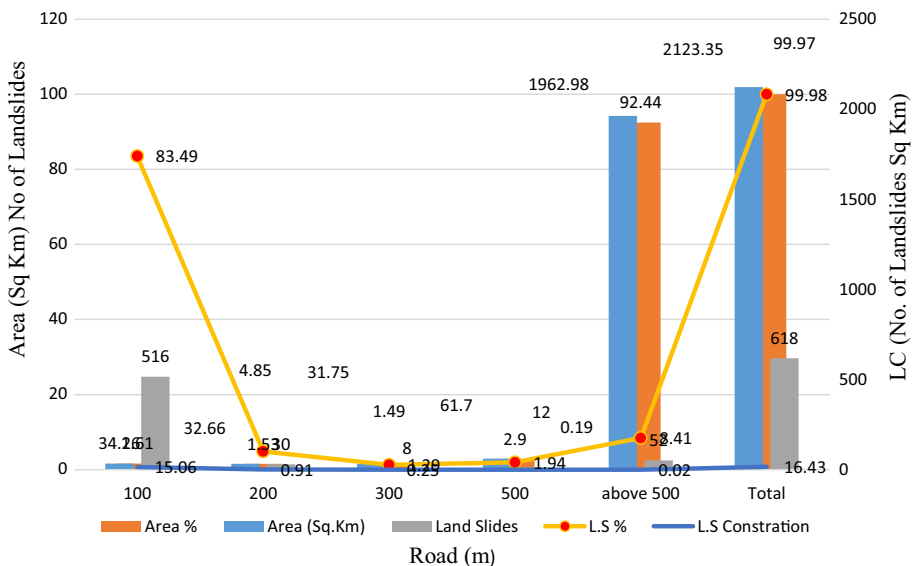


Fig. 20 Spatial distribution analysis of landslides with respect to distance from road network

In this method, a landslide inventory by the combination of Google Earth imageries and field identifications of the study area was established, and then identification and development of causative factors were established that influence the landslides (Shafique et al. 2016). By the overlay of landslides inventory with each causative factor map, landslide (Keefer 1984) distribution maps are prepared and analyzed in ArcGIS. And finally, the results are illustrated in tabular and graphical form for better interpretation and analysis.

A total of seven causative parameters were identified and developed including elevation, aspect, slope, curvature, lithology, and distance to drainage network and distance to the road network (Shahabi et al. 2015). Topographic factors like slope, aspect, elevation, etc. were derived from (SRTM) DEM of 12.5 m resolution using ArcGIS.

All these seven causative factors were rasterized and were used to calculate the area covered by each feature class and number of landslides present in the class to calculate the landslide concentration (LC). LC determines the^o of severity of landslides and enumerates landslide intensity in a specific feature class of a causative factor (Carrara et al. 1999).

The slope gradient is a highly influencing causative factor for landslide (Chau et al. 1998) triggering in the study area. About 33% of the total landslides occur at a slope angle of 21–30°. Followed by the slope angle of 31–40° in which 29.77% of landslides are lying. Kamp et al. (2008) also concluded that slope gradient influence in triggering of landslides, and they concluded that the majority of landslides occurred at slope between 25–35° in Kashmir earthquake regions. But here in the study area, the slope class of 21°–30° is susceptible to land sliding in future as the majority of landslide frequency is occupied by this most dominating slope class.

Among all factors, the highest landslide concentration (0.478) lies in slope of 0–10°. LC value of other slope classes is as follows: 11°–20° (0.371), 21°–30° (0.378), 31°–40° (0.248), 41°–50° (0.180), 51°–60° (0.330), 61°–70° (0.291), and 71°–80° (0).

The second highest LC value (15.058) is of first 100 m zone around road network. Buffer zones are developed having increasing an intervals from the road network, having an interval of 100 m, 200 m, 300 m, 500 m, and more than 500 m. In the first 100 m buffer, landslide concentration is 15.058% and 83.49% of the total landslides occurs in this category, in the next zone of 200 m, it declines to 0.918 and 4.85% of the landslides occurs in this category. In the next 300 m, it decline to 0.25. In next zone of 500 m, LC values further reduce to 0.194 to possessing 1.94% of the total landslides. In the zone of more than 500 m, it slightly increases to 0.02.

The occurrence of 83.49% of total landslides in just the first 100 m zone around the road network and then a gradual decrease on moving away from shows that the factor of human activity has a great dominance for slope destabilization by removing the slope toes which caused land sliding (Maerz et al. 2015).

The third highest LC value is found in the first 100 m around drainage i.e., 4.60. As it is concluded from results that distance to drainage also has an association with landslide occurrence. Drainage causes undercutting during flood seasons so becomes a causative factor for land sliding.

In other zones of drainage (Riaz et al. 2018), LC gradually declines to 1.07 in the 200 m zone, 0.12 in the 300 m zone, and 0.06 in more than 300 m zones. This shows stream networks significantly contributed to slope destabilization in the study area.

In the 2005 Kashmir earthquake, most of the landslides have occurred at a 25 m distance from drainage (Kamp et al. 2008). And in this case maximum landslides (62.78%) also occurred in the first 100 m zone around the drainage network. The Fourth highest landslide concentration, among all causative factors, is found in Alluvial Deposit (0.52), in other rock units, the second highest LC value is found in Glacial Deposit (0.43), in other

rock units, the third highest LC value is found in Tannol Formation (0.37), in other rock units, the fourth LC value is found in Neelum Granite (0.31), in other rock units, the Fifth LC value is found in Panjal Traps (0.29), in other rock units, the sixth LC value is found in Naniyal Group (0.28), in other rock units, the seventh LC value is found in Surghan Group Unit A (0.23), in other rock units, the eighth LC value is found in Surghan Group Unit C-B (0.22), in other rock units, the ninth LC value is found in Surghan Group Unit B (0.14), in other rock units, the tenth LC value is found in Kundal Shai Group (0.13). While Surghan Group Unit C = A Formation has a low LC value (0).

The Elevation is also a dominant causative factor of landslide occurrence. 36.89% of the total landslide occurs in the elevation of 1014–1500 m. Followed by the elevation of 2000–2500 m in which 31.06% of the landslide occurs. The third prominent class is 1500–2000 m in which 29.12% of the landslide occurs. The highest LC value is found in 4.96 in elevation class of 1014–1500 m. Followed by the elevation of 1500–2000 m (1.08). The third prominent elevation is 2000–2500 m which has a 0.47 LC value. Lower altitudes have more LC value because of their closeness to main streams and road networks of the area (Uzielli et al. 2008).

The Slope aspect is also an important causative factor in slope failures (Soomro et al. 2012). The study area has a diversity of slope orientations. With few exceptions, a more or less equal%age of area is trending in all directions. However, Southeast orienting slopes are a bit greater (14.64% of the total area). The highest LC value (0.55) is found in east orienting. Then LC gradually declines in south (0.50), southeast (0.49), southwest (0.26), northeast (0.19), north (0.08), northwest (0.017), and west (0.016). East oriented slopes have high landslide occurrence because of a bit longer exposure to sunlight that gives rise to alternate freezing and melting of water especially in winter causing slope destabilization (Freeman et al. 2002).

Landslide distribution analysis concerning curvature of the area reveals that the majority of the landslides (70.87%) are occurring in convex curvature, while 29.12% of the landslides is occurring in concave curvature. Most of the study area (81.67%) also lies in convex curvature and 18.32% of the study area lies in concave curvature. LC value is high (0.46) in the concave slope as compared to that of the convex slope (0.25).

The Landslide classification map is also prepared on field observation which shows that debris slides are 57.54% of total landslides, followed by the rock slide (18.84%), debris fall (13.76%), and rock fall (10.14). The highest dominance of debris slides shows that the majority of the area possesses weathering product of loose materials as a form of regolith which is easily dislocated by causative factors in a form of debris slides (Haines et al. 2006).

6 Conclusions

This research work applied landslide spatial distribution analysis to measure landslide characteristics for district Neelum, Azad Jammu and Kashmir, Pakistan.

The slope range of 21–30° is more vulnerable to landslide occurrence due to its dominance and high frequency of landslides. Besides, an LC value of 0.47 is found in the slope class of 0–10°. The elevation range of 1014–1500 m contains the majority of total landslides i.e., 36.89%. And the LC value of 4.96 is also high in this class. The First 100 m buffer zone around the road network possesses about 83.49% of the total landslide, and the LC value is significantly high (15.05) in this zone. The First 100 m buffer zone around

drainage possesses 62.78% of the total landslides, and landside concentration is also high (4.60) in this zone. The LC varies between different lithological units. However, LC is high in quaternary deposits. Landslide frequency and LC value are a bit higher in the east direction as compared to other orientations. The most dominant type of landslide is debris slide (57.54%), followed by the rock slide (18.84%), debris fall (13.76%), and rock fall (10.14).

References

- Abbasi A, Khan MA, Ishfaq M, Mool PK (2002) Slope failure and landslide mechanism in Murree area, North Pakistan. *Geol Bull Univ Peshawar* 35:125–137
- Agliardi FN et al (2009) Integrating rockfall risk assessment and countermeasure design by 3D modelling techniques. *Natural Hazards Earth Syst Sci* 9(4):1059
- Ali FN et al (2017) Structural and climatic control of mass movements along the karakoram highway. *Advancing culture of living with landslides*. Springer, Cham, pp 509–516
- Ayalew L, Yamagishi H (2005) The application of GIS-based logistic regression for landslide susceptibility mapping in the Kakuda-Yahiko Mountains. *Central Japan Geomorphology* 65(1–2):15–31
- Ayalew L, Yamagishi H, Ugawa N (2004) Landslide susceptibility mapping using GIS-based weighted linear combination, the case in Tsugawa area of Agano River, Niigata Prefecture. *Japan Landslides* 1(1):73–81
- Baig MS, Lawrence RD (1987) Precambrian to Early Paleozoic orogenesis in the Himalaya. *Kashmir Journal of Geology* 5:1–22
- Barredo FN et al (2000) Comparing heuristic landslide hazard assessment techniques using GIS in the Tirajana basin, Gran Canaria Island, Spain. *Int J Appl Earth Obs Geoinf* 2(1):9–23
- Basharat M (2012) The distribution, characteristics and behaviour of mass movements triggered by the Kashmir Earthquake 2005. NW Himalaya, Pakistan
- Basharat M, Rohn J (2015) Effects of volume on travel distance of mass movements triggered by the 2005 Kashmir earthquake, in the Northeast Himalayas of Pakistan. *Nat Hazards* 77(1):273–292
- Bibi FN et al (2016) Landslide susceptibility assessment through fuzzy logic inference system (flis). *Int Arch Photogramm Remote Sens Spat Info Sci* 42:355
- Bouhadad Y, Benhamouche A, Bourenane H, Ouali AA, Chikh M, Guessoum N (2010) The Laalam (Algeria) damaging landslide triggered by a moderate earthquake ($M_w = 5.2$). *Nat Hazards* 54(2):261–272
- Brawner and Wyllie (1976). Rock slope stability on railway projects. *Area Bulletin*, 77(Bulletin 656).
- Buss K et al. (1995) Highway rock slope reclamation and stabilization, black hills region, South Dakota, Part II, guidelines. Final Report.
- Calkins JA, et al. (1975) Geology of the southern Himalaya in Hazara, Pakistan, and adjacent areas. US Govt. Print. Off
- Carrara A, Guzzetti F, Cardinali M, Reichenbach P (1999) Use of GIS technology in the prediction and monitoring of landslide hazard. *Nat Hazards* 20(2–3):117–135
- Chau FN et al (1998) Rockfall problems in Hong Kong and some new experimental results for coefficients of restitution. *Int J Rock Mech Min Sci* 35(4–5):662–663
- Cruden DM, Varnes DJ (1996) Landslide types and processes in Landslides: investigation and mitigation. In: Turner AK, Schuster RL (Ed), *Transportation Research Board, Special Report No. 247*, p. 36–75
- Cruden, D. M. & Varnes, D. J. (1996). *Landslides: investigation and mitigation*. Chapter 3-Landslide types and processes. *Transportation Research Board Special Report*, p. 247.
- Freeman P (2002) *Catastrophes and development: Integrating natural catastrophes into development planning*.
- Greco A (1989) The crystalline rocks of the Kaghan Valley (NE-Pakistan). *Eclogae Geologicae Helvetiae* 82:629–653
- Haines FN et al (2006) Climate change and human health: impacts, vulnerability and public health. *Public Health* 120(7):585–596
- Hewitt K (1999) Quaternary moraines vs catastrophic rock avalanches in the Karakoram Himalaya, northern Pakistan. *Quatern Res* 51(3):220–237
- Highland L, Bobrowsky PT (2008) *The landslide handbook: a guide to understanding landslides*. US Geological Survey Reston.
- Hussain A, Khan MR, Malik NA, Amin M, Shah MH, Tahir MN (2017) GIS based mapping and analysis of landslide hazard's impact on tourism: a case study of Balakot valley, Pakistan.

- Hutchinson JH (1988) General report, morphological and geotechnical parameters of landslides in relation to geology and hydrogeology. In: Landslides, Proceedings of the Fifth International Symposium on Landslides, 1988.
- Jadoon IAK, Hinderer M, Kausar AB, Qureshi AA, Baig MS, Basharat M, Frisch W (2015) Structural interpretation and geo-hazard assessment of a locking line: 2005 Kashmir Earthquake, western Himalayas. *Environ Earth Sci* 73(11):7587–7602
- Kamp U, Growley BJ, Khattak GA, Owen LA (2008) GIS-based landslide susceptibility mapping for the 2005 Kashmir earthquake region. *Geomorphology* 101(4):631–642
- Kanwal FN et al (2017) GIS based landslide susceptibility mapping of northern areas of Pakistan, a case study of Shigar and Shyok Basins. *Geomat Nat Hazards Risk* 8(2):348–366
- Keefer DK (1984) Landslides caused by earthquakes. *Geol Soc Am Bull* 95(4):406–421
- Khan AN (2000) Landslide hazard and policy response in Pakistan: a case study of Murree. *Pakistan Sci Vis* 6(1):35–48
- Kiani MJ, Abbasi MK, Rahim N (2005) Use of organic manure with mineral N fertilizer increases wheat yield at Rawalakot Azad Jammu and Kashmir. *Archiv Agron Soil Sci* 51(3):299–309
- Soomro et al. (2012). A Conceptual Model for identifying Landslide risk: A case study Balakot, Pakistan. *Sindh University Research Journal-SURJ (Science Series)*, 44(2).
- Maerz FN et al (2015) Remediation and mitigation strategies for rock fall hazards along the highways of Fayfa Mountain, Jazan Region, Kingdom of Saudi Arabia. *Arab J Geosci* 8(5):2633–2651
- Mughal MS, Khan MS, Khan MR, Mustafa S, Hameed F, Basharat M, Niaz A (2016) Petrology and geochemistry of Jura granite and granite gneiss in the Neelum Valley, Lesser Himalayas (Kashmir, Pakistan). *Arab J Geosci* 9(8):528
- Naseer S, Ahmad D, Hussain Z (2019) Petrographic, physical and mechanical properties of sandstone of mirpur district area state of AJ&K. *Pakistan Earth Sci Malaysia* 3(2):32–38
- Nefeslioglu HA, Gokceoglu C, Sonmez H (2008) An assessment on the use of logistic regression and artificial neural networks with different sampling strategies for the preparation of landslide susceptibility maps. *Eng Geol* 97(3–4):171–191
- Norini G et al (2016) (2016). Delineation of alluvial fans from digital elevation models with a GIS algorithm for the geomorphological mapping of the Earth and Mars. *Geomorphology* 273:134–149
- Owen LA, Kamp U, Khattak GA, Harp EL, Keefer DK, Bauer MA (2008) Landslides triggered by the 8 October 2005 Kashmir earthquake. *Geomorphology* 94(1–2):1–9
- Petley D, Dunning S, Rosser N, Kausar AB (2006) Incipient landslides in the Jhelum Valley, Pakistan following the 8th October 2005 earthquake. *Messages V*.
- Pierson LA et al. (1993) *Rockfall hazard rating system-participants' manual*.
- Regmi FN et al (2016) Rock fall hazard and risk assessment along Araniko Highway. Central Nepal Himalaya *Environ Earth Sci* 75(14):1112
- Riaz MT, Basharat M, Hameed N, Shafique M, Luo J (2018) A data-driven approach to landslide-susceptibility mapping in mountainous terrain: Case study from the northwest himalayas, Pakistan. *Nat Hazard Rev* 19(4):5018007
- Romana M (1985) New adjustment ratings for application of Bieniawski classification to slopes. In: Proceedings of the International Symposium on Role of Rock Mechanics, Zacatecas, Mexico, p. 49–53.
- Sandyavutri A (2016) Developing and selecting slope stabilization techniques in managing slope failures. *Jurnal Teknik Sipil* 12(4)
- Sarwar FN et al (2016) Earthquake Statistics and Earthquake Research Studies in Pakistan. *Open Journal of Earthquake Research* 5(02):97
- Sato HP et al (2007) Interpretation of landslide distribution triggered by the 2005 Northern Pakistan earthquake using SPOT 5 imagery. *Landslides* 4(2):113–122
- Sato HP, Hasegawa H, Fujiwara S, Tobita M, Koarai M, Une H, Iwahashi J (2007) Interpretation of landslide distribution triggered by the 2005 Northern Pakistan earthquake using SPOT 5 imagery. *Landslides* 4(2):113–122
- Shafique M, van der Meijde M, Khan MA (2016) A review of the 2005 Kashmir earthquake-induced landslides: from a remote sensing prospective. *J Asian Earth Sci* 118:68–80. <https://doi.org/10.1016/j.jseas.2016.01.002>
- Shahabi H, Hashim M, Ahmad BB (2015) Remote sensing and GIS-based landslide susceptibility mapping using frequency ratio, logistic regression, and fuzzy logic methods at the central Zab basin. *Iran Environmental Earth Sciences* 73(12):8647–8668
- Sudmeier-Rieux K, Qureshi RA, Peduzzi P, Jaboyedoff MJ, Breguet A, Dubois J, Jaubert R, Cheema MA (2007) An interdisciplinary approach to understanding landslides and risk management: a case study from earthquake-affected Kashmir. *Mountain Forum, Mountain GIS e-Conference*, January 14–25, 2008.

- Taherynia MH et al (2014) Assessment of slope instability and risk analysis of road cut slopes in Lashotor Pass, Iran. *J Geol Res* 2014:1–12
- Tan Q, Wang P, Hu J, Zhou P, Bai M, Hu J (2020) The application of multi-sensor target tracking and fusion technology to the comprehensive early warning information extraction of landslide multi-point monitoring Data. *Measurement* 166:108044
- Uzielli FN et al (2008) A conceptual framework for quantitative estimation of physical vulnerability to landslides. *Eng Geol* 102(3–4):251–256
- Wadia DN (1931) The syntaxis of the northwest Himalaya: Its rocks, tectonics and orogeny. *Records Geol Survey India* 65:189–220
- Waseem M, Lai CG, Spacone E (2018) Seismic hazard assessment of northern Pakistan. *Nat Hazard* 90(2):563–600. <https://doi.org/10.1007/s11069-017-3058-1>
- Xu C, Xu X, Shyu JBH, Zheng W, Min W (2014) Landslides triggered by the 22 July 2013 Minxian-Zhangxian, China, Mw 5.9 earthquake: inventory compiling and spatial distribution analysis. *J Asian Earth Sci* 92:125–142
- Yalcin A, Reis S, Aydinoglu AC, Yomralioglu T (2011) A GIS-based comparative study of frequency ratio, analytical hierarchy process, bivariate statistics and logistics regression methods for landslide susceptibility mapping in Trabzon. *NE Turkey Catena* 85(3):274–287
- Zhou Q, Xu Q, Peng D, Fan X, Ouyang C, Zhao K, Li H, Zhu X (2020) Quantitative spatial distribution model of site-specific loess landslides on the Heifangtai terrace, China. *Landslides*. <https://doi.org/10.1007/s10346-020-01551-y>

Publisher's Note Springer Nature remains neutral with regard to jurisdictional claims in published maps and institutional affiliations.